

# A Retrospective Respiratory Gating System Based on Epipolar Consistency Conditions

Maosen Lian<sup>1</sup>, Yi Li<sup>1</sup>, Xiaohui Gu<sup>1</sup> and Shouhua Luo<sup>1,\*</sup>

<sup>1</sup>School of Biological Science and Medical Engineering, Southeast University, NanJing, China

\*Corresponding Author: Shouhua Luo. Email: luoshouhua@seu.edu.cn

Received: 15 May 2019; Accepted: 10 August 2019.

**Abstract:** Motion artifacts of *in vivo* imaging, due to rapid respiration rate and respiration displacements of the mice while free-breathing, is a major challenge in micro computed tomography (micro-CT). The respiratory gating is often served for either projective images acquisition or per projection qualification, so as to eliminate the artifacts brought by *in vivo* motion. In this paper, we propose a novel respiratory gating method, which firstly divides one rotation cycle into a number of segments, and extracts the respiratory signal from the projective image series of current segment by the value of the epipolar consistency conditions (ECC), then in terms of the measured average respiratory period, sets next segment's start-up time and rotation speed of the gantry for respiratory phase synchronization, and so on so forth. The gating procedure is through the whole projections of three cycles, only one among three projections at each angle is qualified by their phase value and is retained for future use for tomographic image reconstruction. In practical experiment, the ECC based gating method and the conventional hardware gating method are employed on micro CT imaging of C57BL/6 mice respectively. The result shows that, compared with the hardware based one, the proposed method not only achieve much better consistency in the projection images, but also suppresses the streak artifacts more effectively on the different parts like the breast, abdomen and head of *in vivo* mice.

**Keywords:** Respiratory gating system; epipolar consistency conditions

## 1 Introduction

Due to its high spatial resolution, Micro CT is usually as the first choice for lung imaging in preclinical study [1,2]. As the rotation time of micro-CT gantry is much slower and the respiration rate of small animal is higher, it is difficult to apply clinical CT gating techniques to micro-CT directly. In clinic, by rapid gantry rotation and patient breath holding, the clinical CT are capable to collect the complete data in one respiratory cycle, while in micro CT system, the whole time for those usually takes hundreds and thousands small animal respiratory cycles, motion artifacts brought by respiratory cycles are inevitably introduced in reconstructed images.

Respiratory gating is an effective way to resolve the problem of motion artifacts. As the acquisition schemes of the prospective gating requires that the projected data at each angle is at the same respiratory phase [3], it will take longer exposure time accordingly, although the reconstructed image can achieve better spatial resolution thereafter. Owing to the damage caused by X-ray radiation to organisms, the longer exposure time of prospective respiratory gating leads to high dose, which may have a great harm on animal health in longitudinal studies. On the contrary, the exposure time of the retrospective respiratory gating is greatly reduced by continuous capturing, only step need to be taken further is to discriminate the respiratory phase of projection during image reconstruction.



This work is licensed under a Creative Commons Attribution 4.0 International License, which permits unrestricted use, distribution, and reproduction in any medium, provided the original work is properly cited.

No matter how a variety of respiratory gating methods, respiratory monitoring is always playing a key role. There are two ways for implementing respiratory monitoring of small animal breathing: invasive or non-invasive. Although invasive measures of ventilation by endotracheal intubation can yield a respiratory signal [4], it may cause physical injury in animals. Meanwhile, some studies have proposed non-invasive monitoring system with or without body surface markers to obtain respiratory signal, where the respiratory signal can be achieved either from a region of interest in the diaphragm [5,6], or from ECC metric among projections [7]. In the previous one, the body surface markers only can be placed on the lung part of small animal, while the later one is suitable for any projections of body parts affected by breathing motion.

In this paper, a new respiratory gating system based on ECC is proposed to reduce respiratory artifacts. This gating system uses ECC to extract respiratory signal and adjust the system accordingly. In Section 2, the principle of collecting respiratory signal by ECC metric is introduced, and the detail of respiratory gating system is described. In Section 3, the experiment results on reconstruction are performed. Finally, the representative results are discussed, and the conclusion is drawn.

## 2 Structure

### 2.1 Respiratory Signal Extraction based on Epipolar Consistency Conditions

As illustrated in Fig. 1,  $s_0$  and  $s_1$  are two points at the source trajectory. The connection line between  $s_0$  and  $s_1$  is named the baseline. The fan beams, which are from  $s_0$  and  $s_1$  and through object plane (denoted as the epipolar plane E), are projected to the corresponding detector plane, forming a pair of epipolar line ( $l_0$  and  $l_1$ ).

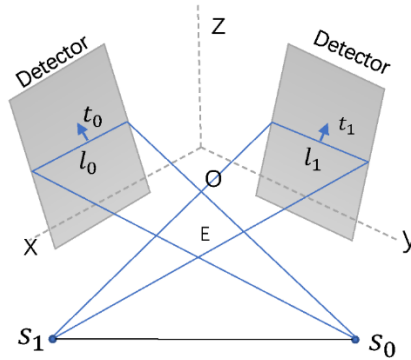


**Figure 1:** Epipolar geometry in cone beam CT

We use the epipolar geometry in cone beam CT to obtain the epipolar line and calculate line integration ( $SX_f$ ). Aichert et al. [8] use Grangeat's theorem [7] to prove that the partial derivative in t-direction of the integration of the epipolar line pair ( $l_0$  and  $l_1$ ) to t are approximately equal. That is

$$\frac{\partial}{\partial t} SX_f(l_0) - \frac{\partial}{\partial t} SX_f(l_1) \approx 0 \quad (1)$$

where t is the distance of the line to the image origin.

The Eq. (1) denotes that the geometric consistency can be quantified by the epipolar line pairs between two projection. Defining k as the angle between the epipolar plane and the xoy plane, the different epipolar line pairs will be found when altering k, which has the same relation as Eq. (1). Luo et al. [9] takes all epipolar line pairs into account with Euclidean style sampling method and define the epipolar consistency conditions metric as:

$$M(l_0, l_1) = \sum_k (\frac{\partial}{\partial t} SX_f(l_0) - \frac{\partial}{\partial t} SX_f(l_1))^2 / C_k \quad (2)$$

where  $C_k$  denotes the total number of the epipolar line pairs.

In one breathing cycle, the respiratory signal after gas anesthesia can be divided into 2 parts: the respiratory resting period and excited period. The resting period can hold for several seconds without

obvious organ motions and projection inconsistency, thus the ECC value  $M$  among the projection images over the period will be small. In the respiratory excited period, the ECC value  $M$  will increase with the thoracic contraction until reaching the peak of respiration, then decrease with the thoracic diastole. Hence, if we take an projection image in the resting period as the reference image  $I_{ref}$ , the ECC value between  $I_{ref}$  and all other projections ( $I_0, I_1 \dots I_i$ ) in the sequence can be made (Eq. (3)), and then all those value vs. the number of sequence can make the respiration waveform, as is shown in Fig. 2.

$$F(I_0, I_1 \dots I_i) = (M(I_{ref}, I_0), M(I_{ref}, I_1) \dots, M(I_{ref}, I_i)) \tag{3}$$

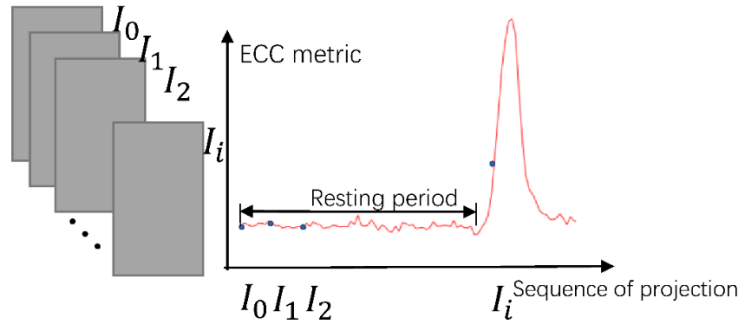


**Figure 2:** Express ECC metric of projections as respiratory signal

If we implement the Eq. (3) in practice, the big issue is that it is unknown when the resting period is taking place, thus the reference image  $I_{ref}$  cannot be selected in advance. We tend to summarize all ECC value between each one in the sequence and all others, as is shown in Eq. (4).

$$F(I_0, I_1 \dots I_i) = (\sum_{k \neq 0} M(I_k, I_0), \sum_{k \neq 1} M(I_k, I_1), \dots, \sum_{k \neq i} M(I_k, I_i) ) \tag{4}$$

Though the Eq. (4) is more computationally intensive than the Eq. (3), it is practicable in the actual situation while dismissing the unknown resting period issue.

The Fig. 3(a) shows the magnitude of ECC value obtained by Eq. (4) from part of the projections of one mouse after the gas anesthesia. The respiratory phase (Fig. 3(b)) is made by the following way: The phase value is defined as 0 from a peak of Fig. 3(a), as 1.0 at the following next peak. The phase value of two peaks are linearly distributed between 0-1. As illustrated in Fig. 3, the red dots in the Fig. 3(a) correspond to those phase values fall in between 0.2 to 0.8 in Fig. 3(b), and the blue dots phase value are others. In fact, part of projections transit from existed period to resting period. According to experience, the projections selected by phase values only in 0.2 to 0.8 are positively identified as resting projection.

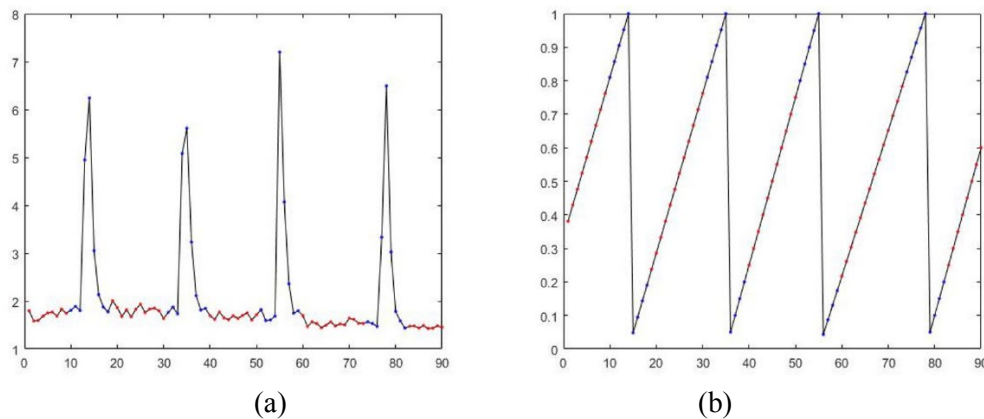


**Figure 3:** The waveform of the ECC value vs. the projection sequence. The magnitude of ECC value (a), its phase (b)

## 2.2 Retrospective Respiratory Gating

In this retrospective gating, the acquisition system needs to handle the number of the segment, the rotating speed and starting time of the gantry constantly, to optimize the adequate period over different angles. Each time the respiratory signal is made by Eq. (4).

At the beginning, the gantry performs a 30-degree scanning, and then the initial rotation speed is estimated by the current respiratory cycle. Afterwards, a whole 360 degrees scanning is divided into several scanning segment with equal angle. In order to acquire a similar number of resting phase projections in each breathing cycle, the rotating speed ( $v$ ) of every next segment will be adjusted by the average breathing cycle ( $T_B$ ) of the last segment. When the breathing cycle is shorter, the rotation speed of gantry slows down, and vice versa, as is depicted in the Eq. (5).

$$v = \frac{N}{T_B \cdot C} \quad (5)$$

where  $N$  denotes total number of angles of each segment, and  $C$  is constant.

The projection of each angle for reconstruction should come from the resting phase essentially. Since the gantry is always rotating continuously in one direction, there are inevitably some projections that fall into the respiratory excited period. Therefore, streak artifacts brought by the organ moving come very naturally in *in-vivo* CT images. To address this problem, it requires at least two laps of the gantry rotation theoretically. By synchronizing each segment, the breathing waveform at each angle can be swapped such that one projection at same angle falls into the resting phase at least one time in two laps. Additionally, in view of mice respiratory twitch, it is better for having three laps totally in our implementation, over 600 projection images are acquired at each lap respectively. For each segment in  $i^{th}$  lap, the start-up time  $T_i$  is adjusted by the following Eq. (6).

$$T_i = [T_C/T_B] \cdot T_B + i * \frac{T_B}{2} - T_C + T_E \quad (6)$$

where  $T_C$  denotes the whole time of calculating ECC value,  $T_B$  is breathing period and  $T_E$  is the end time of segment scanning.

If the breathing cycle by Eq. (4) is not calculated accurately enough, it turns out that all three projections at one angle may not fall into the resting phase. In this case, the best one for reconstruction depends on whose phase value is closest to the range of the resting phase. The whole algorithm is depicted as below:

---

### PSEUDO-CODE FOR RESPIRATORY GATING BASED ON ECC

---

1. Initialize: rotate 30° and scan
  2. Calculate breathing cycle
  3. Divide a circle into  $K$  segments, and set rotation speed by Eq. (5)
  4. For  $i=1$  to 3 laps do
    5. For  $k=1$  to  $K$  segments do
      6. Delay relying on Eq. (6)
      7. Rotate and scan
      8. Calculate breath period using ECC method
      9. Change the speed by Eq. (5)
    10. End For
  11. End For
  12. Integrate a circle of projections in any angle relying on the respiratory phase
  13. Use total projections of integrated circle to reconstruct images by FDK algorithm [10]
-

### 3 Results

In the experiment, two types of respiratory gating are given: the ECC based and hardware based. The hardware-based gating, as shown in the Fig. 4, conventionally stick a marker (Fig. 4(a)) on the lungs portion of the mice, extracting respiratory signal via a miniature camera (Fig. 4(c)) when the body moving. The breathing mask (Fig. 4(b)) provides isoflurane and oxygen to mouse. The respiratory waveform (Fig. 5) is composed by the centroid displacements of the surface marker.

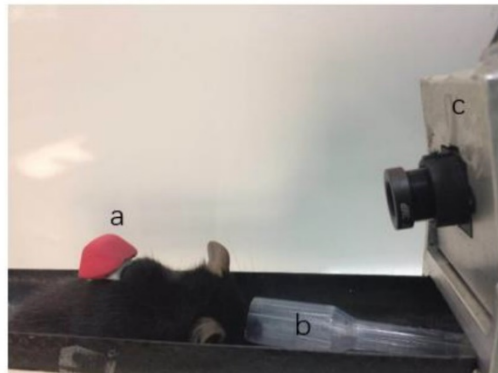


**Figure 4:** Hardware based gating. (a) The red marker, (b) the breathing mask, (c) the miniature camera

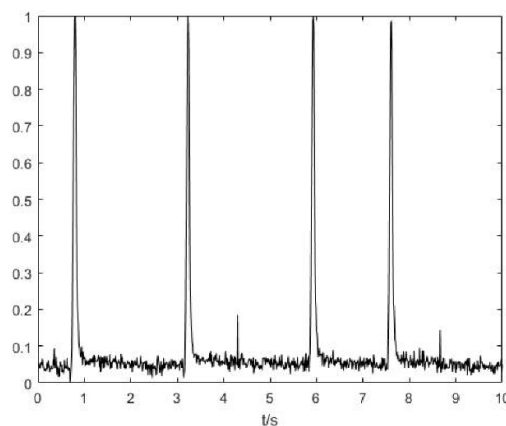


**Figure 5:** Respiratory waveform calculated by hardware-based gating. x label is time, y is value of the normalized centroid displacement

In order to slow down the breathing rate of C57BL/6 mice, they are anesthetized with the gas consisting of isoflurane and oxygen, and then the projection images are acquired continuously by two gating systems respectively. In our experiment, the scanning parameters of Micro CT system are set as follows: tube voltage: 60 kV, tube current: 120 uA, exposure time: 50 ms. Three groups of experiment were carried out: the head, chest and abdomen imaging of one C57BL/6 mice respectively. Some common characteristics in actual experiments show that, the movement of the thorax is always transmitted to the abdomen, creating a weak movement therein; and the mice undergoing the isoflurane anesthesia gasp dramatically from nose to mouth, causing periodic head shaking.

Figs. 6-8 show the suppression effect of motion artifacts by two types of gating. In each figure, the first row (a1-a3) is the reconstruction result without any respiratory gating, the second row (b1-b3) is the reconstruction result with hardware-based gating, and the last row (c1-c3) is the result with ECC based gating. Each row of figure consists of three results (1-3) at different transactional positions. The arrows in each figure mark the area affected by respiratory artifact. Compared with first and second row in the thoracic abdominal and head reconstruction, although the most artifacts in first row have been suppressed by hardware-based gating, some streak artifacts are still obvious in hardware-based results. From the results

of ECC-based gating, the artifacts have been visually removed. It demonstrates that the ECC based gating are superior on reducing respiratory artifacts than the hardware based one.

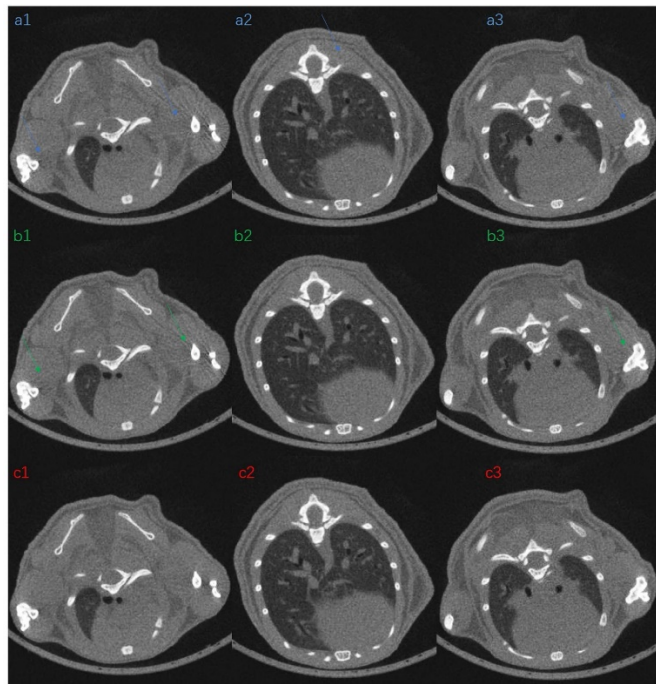


**Figure 6:** Thoracic imaging without gating (a1-a3) and by hardware-based gating (b1-b3) and ECC-based gating (c1-c3), the arrows indicate the area affected by respiratory artifact

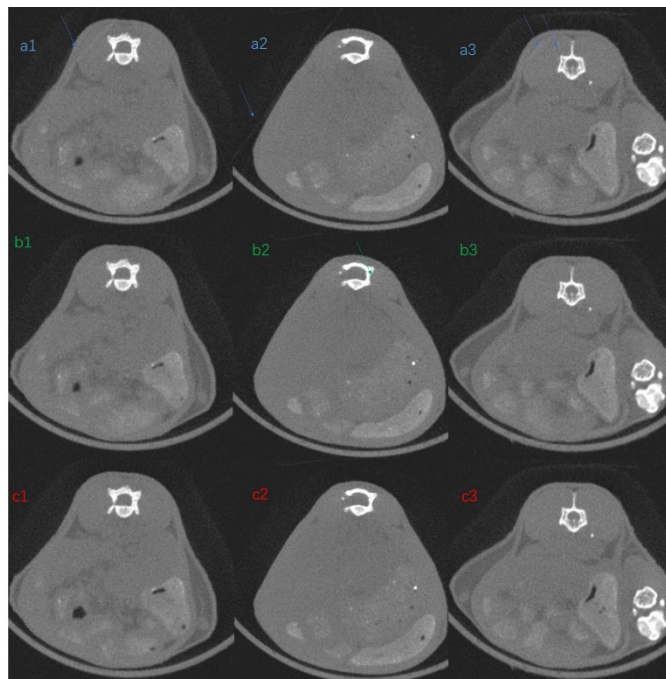


**Figure 7:** Abdominal imaging without gating (a1-a3) and by hardware-based gating (b1-b3) and ECC-based gating (c1-c3), the arrows indicate the area affected by respiratory artifact

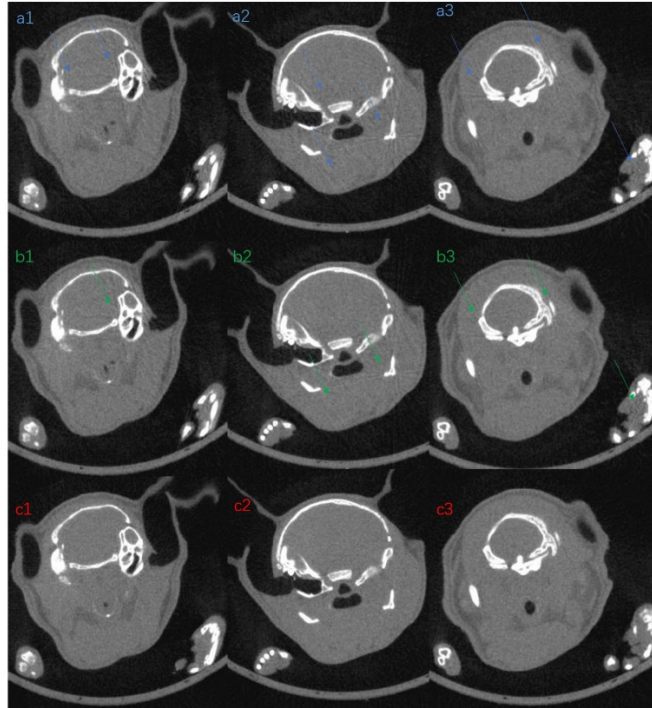


**Figure 8:** Head imaging without gating (a1-a3) and by hardware-based gating (b1-b3) and ECC-based gating (c1-c3), the arrows indicate the area affected by respiratory artifact

The tri-laps' projections collected by the gating system only leaves one for each angle. The extent to which these selected projections are affected by motion can be evaluated by the ECC metric. Fig. 9 shows the epipolar consistency curves of three groups of the experimental projections. The blue line is the ECC values without respiratory gating, as the same time the line describes as the respiratory motion under anesthetized. The green line represents ECC of projections from the hardware gating, while the red line represents those from the ECC based gating. From left to right in Fig. 9, the ECC variances of the projections with hardware gating is 0.0091, 0.3234 and 0.0894 respectively, while those with the ECC gating is 0.0035, 0.0029 and 0.0015. It demonstrates that, from this perspective, the ECC based gating is better than the hardware gating method.

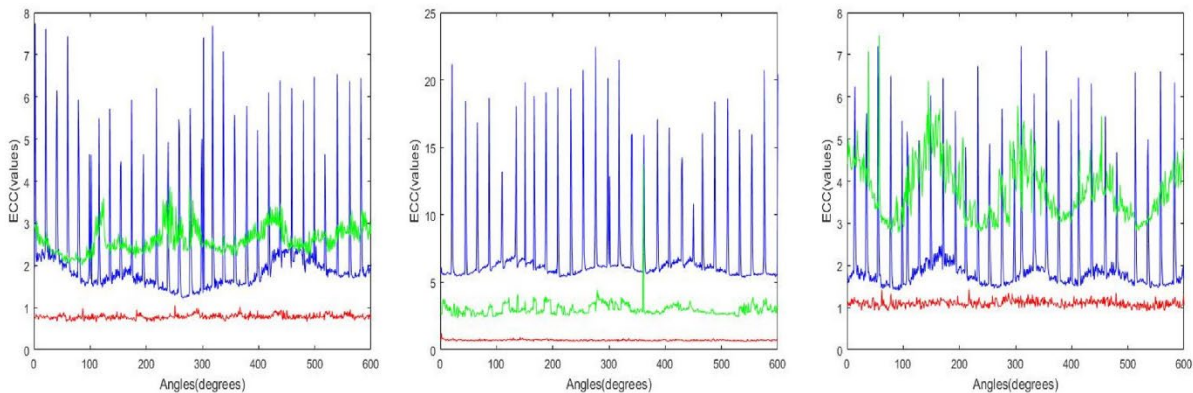


**Figure 9:** The ECC curves of the projections without gating and with two gating system. (a) Thoracic ECC, (b) Abdominal ECC, (c) Head ECC

#### 4 Conclusion

Respiratory artifact is one of the most common artifacts in *in-vivo* imaging of micro-CT. Respiratory gating methods are always employed to suppress these kinds of artifacts. In this paper, we design a retrospective respiratory gating system based on epipolar consistency conditions. Compared with the hardware based one, the ECC based gating takes the respiratory signal from the acquired projections directly, the imaging process does not require any additional hardware, thus the whole procedure for *in-vivo* imaging is more easy and faster. The real experiment results show that the ECC based gating has a better performance in reducing respiratory artifacts in different body parts, such as head, abdominal and thorax of mouse. Furthermore, in terms of epipolar consistency of projection, retrospective respiratory gating based on ECC also outperforms than the hardware gating.

**Acknowledgement:** This work was supported in part by National Key R&D Program of China (2017YFA0104302) and National Natural Science Foundation of China (61871126).

#### References

1. Schambach SJ, Bag S, Schilling L, Groden C, Brockmann MA. Application of micro-CT in small animal imaging. *Methods* **2010**, 50(1): 2-13.
2. Sapkal PS, Kuthe AM, Ganapathy D, Mathankar SC, Kuthe S. 3D bio-plotted composite scaffold made of collagen treated hydroxyapatite-tricalciumphosphate for rabbit tibia bone regeneration. *Molecular & Cellular Biomechanics* **2016**, 13(2): 131-153.
3. Ford NL, Nikolov HN, Norley CJ, Thornton MM, Foster PJ. et al. Prospective respiratory-gated micro-CT of free breathing rodents. *Medical Physics* **2005**, 32(9): 2888.
4. Cavanaugh D, Johnson E, Price RE, Kurie J, Travis EL. et al. *In vivo* respiratory-gated micro-CT imaging in small-animal oncology models. *Molecular Imaging* **2004**, 3(1): 55-62.
5. Bartling SH, Dinkel J, Stiller W, Grasruck M, Madisch I et al. Intrinsic respiratory gating in small-animal CT. *European Radiology* **2008**, 18(7): 1375-1384.
6. Hu J, Haworth ST, Molthen RC, Dawson CA. Dynamic small animal lung imaging via a postacquisition respiratory gating technique using micro-cone beam computed tomography 1. *Academic Radiology* **2004**, 11(9): 961-970.
7. Grangeat P. Mathematical Framework of Cone Beam 3D Reconstruction Via the First Derivative of the Radon Transform. Springer Berlin Heidelberg. **1992**.
8. Aichert A, Maass N, Deuerling-Zheng Y, Berger M, Manhart M et al. Redundancies in X-ray images due to the epipolar geometry for transmission imaging. *Third CT Meeting* **2014**: 333-337.
9. Luo S, Luo S. An Epipolar based algorithm for respiratory signal extraction of small animal CT. *Sensing and Imaging* **2018**, 19(1): 4.
10. Feldkamp LA, Davis LC, Kress JW. Practical cone-beam algorithm. *Journal of the Optical Society of America A* **1984**, 1(6): 612-619.